A GENERAL PHASE TRANSITION MODEL FOR VEHICULAR TRAFFIC

S. BLANDIN *, D. WORK †, P. GOATIN ‡, B. PICCOLI §, AND A. BAYEN ¶

Abstract. An extension of the Colombo phase transition model is proposed. The congestion phase is described by a two-dimensional zone defined around a standard fundamental diagram. General criteria to build such a set-valued fundamental diagram are enumerated, and instantiated on several standard fluxes with different concavity properties. The solution to the Riemann problem in the presence of phase transitions is obtained through the design of a Riemann solver, which enables the construction of the solution of the Cauchy problem using wavefront tracking. The free-flow phase is described using a Newell-Daganzo fundamental diagram, which allows for a more tractable definition of phase transition compared to the original Colombo phase transition model. The accuracy of the numerical solution obtained by a modified Godunov scheme is assessed on benchmark scenarios for the different flux functions constructed.

Key words. partial differential equations, hyperbolic systems of conservation laws, macroscopic highway traffic flow model, phase transition, numerical scheme, riemann solver

AMS subject classifications. 35L65, 35F25, 65M12, 90B20, 76T99

1. Introduction. First order scalar models of traffic.

Hydrodynamic models of traffic go back to the 1950's with the work of Lighthill, Whitham and Richards [32, 39], who built the first model of the evolution of vehicle density on the highway using a first order scalar hyperbolic *partial differential equation* (PDE) referred to as the LWR PDE. Their model relies on the knowledge of an empirically measured *flux function*, also called the *fundamental diagram* in transportation engineering, for which measurements go back to 1935 with the pioneering work of Greenshields [22]. Numerous other flux functions have since been proposed in the hope of capturing effects of congestion more accurately, in particular: Greenberg [21], Underwood [44], Newell-Daganzo [10, 35], and Papageorgiou [47]. The existence and uniqueness of an *entropy* solution to the *Cauchy problem* [40] for the class of scalar conservation laws to which the LWR PDE belong go back to the work of Oleinik [36] and Kruzhkov [27], (see also the seminal article of Glimm [18]), which was extended later to the *initial-boundary value problem* [2], and specifically instantiated for the scalar case with a concave flux function in [30], in particular for traffic in [41]. Numerical solutions of the LWR PDE go back to the seminal *Godunov scheme* [20, 31], which was shown to converge to the entropy solution of the first order hyperbolic PDE (in particular the LWR PDE). In the transportation engineering community, the Godunov scheme in the case of a triangular flux is known under the name of *Cell Transmission Model* (CTM), which was brought to the field by Daganzo in 1995 [10, 11] (see [29] for the general case), and is one of the most used discrete traffic flow models in the literature today [5, 13, 24, 33, 34, 37, 46].

*Ph.D. student, Systems Engineering, Department of Civil and Environmental Engineering, University of California, Berkeley, USA. Email: blandin@berkeley.edu. Corresponding author.

†Ph.D. student, Systems Engineering, Department of Civil and Environmental Engineering, University of California, Berkeley, USA. Email: dbwork@berkeley.edu.

‡Research Scientist, EPI OPALE, INRIA Sophia Antipolis Méditerranée, France. E-mail: paola.goatin@inria.fr.

§Professor, Department of Mathematical Sciences, Rutgers University, Camden, USA. Email: piccoli@camden.rutgers.edu

¶Associate Professor, Systems Engineering, Department of Civil and Environmental Engineering, University of California, Berkeley, USA. Email:bayen@berkeley.edu

Set-valued fundamental diagrams. The assumption of a Greenshields fundamental diagram or a triangular *fundamental diagram*, which significantly simplifies the analysis of the model algebraically, led to the aforementioned theoretical developments. Yet, experimental data clearly indicates that while the free flow part of a fundamental diagram can be approximated fairly accurately by a straight line, the congested regime is set valued, and can hardly be characterized by a single curve [45]. An approach to model the set-valuedness of the congested part of the fundamental diagram consists in using a second equation coupled with the mass conservation equation (i.e. the LWR PDE model). Such models go back to Payne [38] and Whitham [48] and generated significant research efforts, but led to models with inherent weaknesses pointed out by del Castillo [15] and Daganzo [12]. These weaknesses were ultimately addressed in several responses [1, 37, 49], leading to sustained research in this field.

Motivation for a new model. Despite the existing research, modeling issues remain in most 2×2 models of traffic available today. For instance, the *Aw-Rascle* model [1] can introduce vanishing velocities below jam density, which is not a classical assumption in traffic theory [17]. In agreement with the remarks from Kerner [25, 26] affirming that traffic flow presents three different behaviors, *free-flow*, *wide moving jams*, and *synchronized flow*, Colombo proposed a 2×2 phase transition model [7, 8] which considers *congestion* and *free-flow* in traffic as two different phases, governed by distinct evolutionary laws (see also [19] for a phase transition version of the Aw-Rascle model). The well-posedness of this model was proved in [9] using *wavefront tracking* techniques [4, 23]. In the phase transition model, the evolution of the parameters is governed by two distinct dynamics; in *free-flow*, the Colombo phase transition model is a classical first order model (LWR PDE), whereas in *congestion* a similar equation governs the evolution of an additional state variable, the *linearized momentum* q. The motivation for an extension of the 2×2 phase transition model comes from the following items, which are addressed by the class of models presented in this article:

(i) *Phases gap.* The phase transition model introduced by Colombo in [7] uses a Greenshields flux function to describe *free-flow*, which despite its simple analytical expression yields a fundamental diagram which is not connected and thus a complex definition of the solution to the Riemann problem between two different phases. We solve this problem by introducing a Newell-Daganzo flux function for *free-flow*, which creates a non-empty intersection between the congested phase and the *free-flow* phase, called *metastable phase*. It alleviates the inconvenience of having to use a shock-like phase transition in many cases to the Riemann problem between two different phases.

(ii) *Definition of a general class of set-valued fundamental diagrams.* The work achieved in [7] enables the definition of a set-valued fundamental diagram for the expression of the velocity function introduced. However, experimental data shows that several types of fundamental diagram exist, with different congested domain shapes. In this article we provide a method to build an arbitrary set-valued fundamental diagram which in a special case corresponds to the fundamental diagram introduced in [7]. This enables one to define a custom-made set-valued fundamental diagram.

Organization of the article. The rest of the article is organized as follows. Section § 2 presents the fundamental features of the Colombo phase transition model [8], which serves as the basis for the present work. In Section § 3, we introduce the modifications to the Colombo phase transition model, and introduce the notion of *standard state* which provides the basis for the construction of a class of 2×2 traffic models. We also assess general conditions which enable us to extend the results obtained for the original Colombo phase transition model to these new models. Finally, this sec-

tion presents a modified *Godunov scheme* which can be used to solve the equations numerically. The two following sections instantiate the constructed class of models for two specific flux functions, which are the Newell-Daganzo (affine) flux function (Section § 4) and the Greenshields (parabolic concave) flux function (Section § 5). Each of these sections includes a discussion of the choice of parameters needed for each of the models, the solution to the Riemann problem, a description of the specific properties of the model, and a validation of the numerical results using a benchmark test. Finally, Section § 6 presents some concluding remarks.

2. The Colombo phase transition model. The original Colombo phase transition model [7, 8] is a set of two coupled PDEs respectively valid in a *free-flow* regime and *congested* regime:

$$\begin{cases} \partial_t \rho + \partial_x(\rho\, v_f(\rho)) = 0 & \text{in free-flow } (\Omega_f) \\ \begin{cases} \partial_t \rho + \partial_x(\rho\, v_c(\rho,q)) = 0 \\ \partial_t q + \partial_x((q-q^*)\, v_c(\rho,q)) = 0 \end{cases} & \text{in congestion } (\Omega_c) \end{cases} \tag{2.1}$$

where the state variables ρ and q denote respectively the density and the *linearized momentum* [8]. Ω_f and Ω_c are the respective domains of validity of the free-flow and congested equations of the model and are explicited below. The term q^* is a characteristic parameter of the road under consideration. An empirical relation expresses the velocity v as a function of density in free-flow: $v := v_f(\rho)$, and as a function of density and linearized momentum in congestion: $v := v_c(\rho, q)$. Following usual choices for traffic applications [16], the functions below are used:

$$v_f(\rho) = \left(1 - \frac{\rho}{R}\right) V \quad \text{and} \quad v_c(\rho, q) = \left(1 - \frac{\rho}{R}\right) \frac{q}{\rho}$$

where R is the maximal density or *jam density* and V is the maximal *free-flow speed*. The relation for free-flow is the *Greenshields* model [22] mentioned earlier while the second relation has been introduced in [7]. Since Ω_c has to be an invariant domain [40] for the congested dynamics from system (2.1), and according to the definition of v, the free-flow and congested domains are defined as follows:

$$\begin{cases} \Omega_f = \{(\rho, q) \in [0, R] \times [0, +\infty[\ \ , v_f(\rho) \geq V_{f-}\ \ ,\ \ q = \rho\, V\} \\ \Omega_c = \left\{(\rho, q) \in [0, R] \times [0, +\infty[\ \ , v_c(\rho, q) \leq V_{c+}\ \ ,\ \ \frac{Q^- - q^*}{R} \leq \frac{q - q^*}{\rho} \leq \frac{Q^+ - q^*}{R}\right\} \end{cases}$$

where V_{f-} is the minimal velocity in free-flow and V_{c+} is the maximal velocity in congestion such that $V_{c+} < V_{f-} < V$. R is the maximal density and Q^- and Q^+ are respectively the minimal and maximal values for q. The fundamental diagram in (ρ, q) coordinates and in $(\rho, \rho\, v)$ coordinates is presented in Figure 2.1.

REMARK 2.1. The congested part of system (2.1) is strictly hyperbolic if and only if the two eigenvalues of its Jacobian are real and distinct for all states $(\rho, q) \in \Omega_c$.

REMARK 2.2. The 1-Lax curves are straight lines going through $(0, q^*)$ in (ρ, q) coordinates which means that along these curves shocks and rarefactions exist and coincide [42]. One must note that the 1-Lax field is not *genuinely non-linear* (GNL). Indeed the 1-Lax curves are *linearly degenerate* (LD) for $q = q^*$ and GNL otherwise with rarefaction waves propagating in different directions relatively to the eigenvectors depending on the sign of $q - q^*$. The 2-Lax curves, which are straight lines going through the origin in $(\rho, \rho\, v)$ coordinates, are always LD.

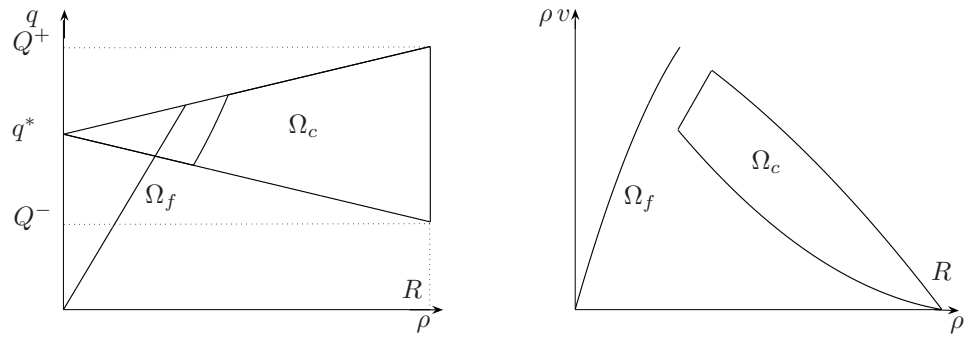

FIG. 2.1. ***Colombo phase transition model. Left**: Fundamental diagram in state space coordinates (ρ, q). **Right**: Fundamental diagram in density flux coordinates $(\rho, \rho\, v)$.*

3. Extension of the Colombo phase transition model. The approach developed by Colombo provides a fundamental diagram which is thick in congestion (Figure 2.1), and thus can model clouds of points observed experimentally (Figure 3.1). We propose to extend this approach by considering the second equation in

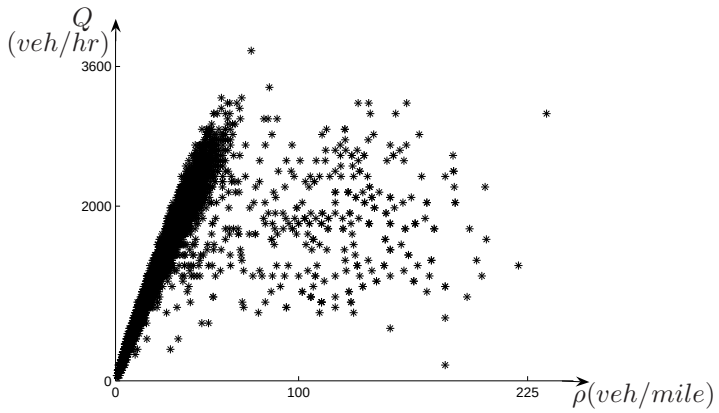

FIG. 3.1. ***Fundamental diagram in density flux coordinates from a street in Rome.** In congestion (high densities) the flux is multi-valued. Count C and velocity v were recorded every minute during one week. Flux Q was computed from the count. Density ρ was computed from flux and velocity according to the expression $Q = \rho\, v$ (see [3] for an extensive analysis of this dataset).*

congestion as modeling a perturbation [49, 50]. The *standard state* (Definition 3.1) would be the usual one-dimensional fundamental diagram, with dynamics described by the conservation of mass. Perturbations can move the system off standard state, leading the diagram to span a two-dimensional area in congestion. A single-valued map is able to describe the free-flow mode, which is therefore completely described by the free-flow standard state.

DEFINITION 3.1. *We call standard state the set of states described by a one dimensional fundamental diagram and the classical LWR PDE. In the following we respectively refer to the standard velocity and standard flux as the velocity and flux at the standard state.*

In this section we present analytical requirements on the velocity function in

congestion which, given the work done in [8], enable us to construct a 2×2 phase transition model. These models provide support for a physically correct, mathematically well-posed initial-boundary-value problem which can model traffic phenomena where the density and the flow are independent quantities in congestion, allowing for multiple values of the flow for a given value of the density. Our framework allows to define the two dimensional zone span by the congestion phase according to the reality of the local traffic nature, which is not always possible with the original Colombo phase transition model.

3.1. Analysis of the standard state. We consider the density variable ρ to belong to the interval $[0, R]$ where R is the maximal density. Given the *critical density* [1] σ in $(0, R]$, we define the standard velocity $v^s(\cdot)$ on $[0, R]$ by:

$$v^s(\rho) := \begin{cases} V & \text{for } \rho \in [0, \sigma] \\ v_c^s(\rho) & \text{for } \rho \in [\sigma, R] \end{cases}$$

where V is the free-flow speed and $v_c^s(\cdot)$ is in $C^\infty((\sigma, R), \mathbb{R}^+)$. It is important to note that $v_c^s(\cdot)$ is a function of ρ only, as it is the case for the classical fundamental diagram. The standard flux $Q^s(\cdot)$ is thus defined on $[0, R]$ by:

$$Q^s(\rho) := \rho\, v^s(\rho) = \begin{cases} Q_f(\rho) := \rho\, V & \text{for } \rho \in [0, \sigma] \\ Q_c^s(\rho) := \rho\, v_c^s(\rho) & \text{for } \rho \in [\sigma, R]. \end{cases}$$

In agreement with traffic flow features, the congested standard flux $Q_c^s(\rho)$ must satisfy the following requirements (which are consistent with the ones given in [14]).

(i) *Flux vanishes at the maximal density*: $Q_c^s(R) = 0$.
This condition encodes the physical situation in which the jam density has been reached. The corresponding velocity and flux of vehicles on the highway is zero.

(ii) *Flux is a decreasing function of density in congestion*: $dQ_c^s(\rho)/d\rho \leq 0$.
This is required as a defining property of congestion. It implies that $dv_c^s(\rho)/d\rho \leq 0$.

(iii) *Continuity of the flux at the critical density*: $Q_c^s(\sigma) = Q_f(\sigma)$.
Even if some models account for a discontinuous flux at capacity, the *capacity drop* phenomenon [26], we assume, following most of the transportation community, that the flux at the standard state is a continuous function of density.

(iv) *Concavity of the flux in congestion*: $Q_c^s(\cdot)$.
The flux function at the standard state $Q_c^s(\cdot)$ must be concave on $[\sigma, \sigma_i]$ and convex on $[\sigma_i, R]$ where σ_i is in $(\sigma, R]$. Given the experimental datasets obtained for congestion (Figure 3.1), it is not clear in practice if the standard flux is concave or convex in congestion. The assumption made here is motivated in Remark 3.14.

REMARK 3.2. In this article we instantiate the general model proposed on the most common standard flux functions, i.e. linear or concave, but the framework developed here applies to flux functions with changing concavity such as the Li flux function [28], although it yields a significantly more complex analysis.

3.2. Analysis of the perturbation.

3.2.1. Model outline. In this section we introduce a perturbation q to the standard velocity in congestion.

[1] Density for which the flux is maximal at the standard state. At this density the system switches between free-flow and congestion.

DEFINITION 3.3. *The perturbed velocity function $v_c(\cdot,\cdot)$ is defined on Ω_c by:*

$$v_c(\rho, q) = v_c^s(\rho)\,(1+q) \tag{3.1}$$

where $v_c^s(\cdot) \in C^\infty((\sigma, R), \mathbb{R}^+)$ is the congested standard velocity function.

The standard state corresponds to $q = 0$, and the evolution of (ρ, q) is described similarly to the classical Colombo phase transition model [8] by:

$$\begin{cases} \partial_t \rho + \partial_x(\rho\, v) = 0 & \text{in free-flow} \\ \begin{cases} \partial_t \rho + \partial_x(\rho\, v) = 0 \\ \partial_t q + \partial_x(q\, v) = 0 \end{cases} & \text{in congestion} \end{cases} \tag{3.2}$$

with the following expression of the velocity:

$$v = \begin{cases} v_f(\rho) := V & \text{in free-flow} \\ v_c(\rho, q) & \text{in congestion.} \end{cases} \tag{3.3}$$

The perturbed velocity function defines the velocity in congestion whereas a Newell-Daganzo function describes the velocity in free-flow. The analytical expression of the free-flow and congested domains as explicited in (3.4) is motivated by the analysis conducted in Table 3.1 and the necessity for these domains to be invariants [40] for the dynamics (3.2) in order to have a well-defined Riemann solver [43].

$$\begin{cases} \Omega_f = \{(\rho, q) \mid (\rho, q) \in [0, R] \times [0, +\infty[\ \ , v_c(\rho, q) = V\ \ ,\ 0 \le \rho \le \sigma_+\} \\ \Omega_c = \left\{(\rho, q) \mid (\rho, q) \in [0, R] \times [0, +\infty[\ \ , v_c(\rho, q) < V\ \ ,\ \frac{q_-}{R} \le \frac{q}{\rho} \le \frac{q_+}{R}\right\} \end{cases} \tag{3.4}$$

σ_+ is defined by $v_c(\sigma_+, \sigma_+\, q_+/R) = V$ and we assume that $V > 0$ and $q_- \le 0 \le q_+$. A definition of the whole set of parameters can be found in Section § 3.3 (See also illustration in Figure 3.2 for the Newell-Daganzo case.).

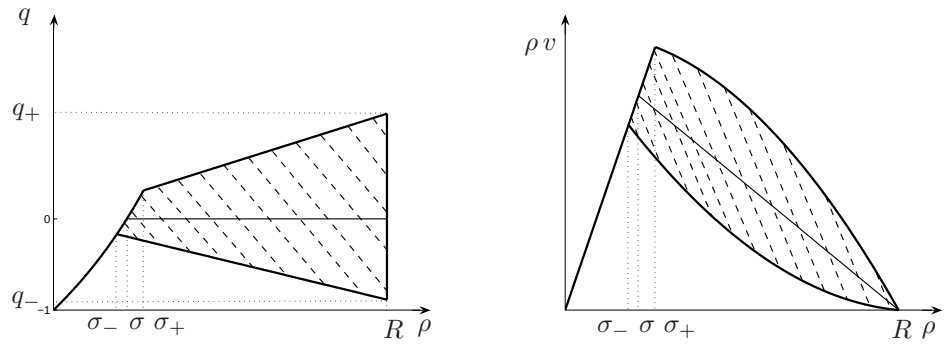

FIG. 3.2. ***Newell-Daganzo standard flux function. Left:*** *Fundamental diagram in state space coordinates.* ***Right:*** *Fundamental diagram in flux-density coordinates. The standard state is the usual triangular diagram. The congestion phase is two-dimensional (striped domain).*

DEFINITION 3.4. *The set $\{(\rho, q) \mid v_c(\rho, q) = V,\ \sigma_- \le \rho \le \sigma_+\}$ defines the metastable phase. This phase defines transition states from the congestion phase to the free-flow phase.*

REMARK 3.5. The left boundary of the congested domain is a convex curve in (ρ, q) coordinates (in Figure 2.1 for the Colombo phase transition model as in Figure 3.2 for the new model derived). Thus Ω_c is not convex in (ρ, q) coordinates.

The analysis of the congestion phase of the model (3.2) is outlined in Table 3.1.

Eigenvalues	$\lambda_1(\rho,q) = \rho\,(1+q)\partial_\rho v_c^s(\rho)+v_c^s(\rho)\,(1+2\,q)$	$\lambda_2(\rho,q) = v_c^s(\rho)\,(1+q)$
Eigenvectors	$r_1 = \begin{pmatrix} \rho \\ q \end{pmatrix}$	$r_2 = \begin{pmatrix} v_c^s(\rho) \\ -(1+q)\,\partial_\rho v_c^s(\rho) \end{pmatrix}$
Nature of the Lax curves	$\nabla\lambda_1.r_1 = \rho^2\,(1+q)\partial^2_{\rho\rho} v_c^s(\rho) + 2\,\rho\,(1+2\,q)\,\partial_\rho v_c^s(\rho) + 2\,q\,v_c^s(\rho)$	$\nabla\lambda_2.r_2 = 0$
Riemann-invariants	q/ρ	$v_c^s(\rho)\,(1+q)$

TABLE 3.1
Congestion phase: *algebraic properties of the general phase transition model.*

3.2.2. Physical and mathematical considerations. Physical interpretation and mathematical conditions translate into the following conditions:

CONDITION 3.6. ***Positivity of speed.*** *In order to maintain positivity of $v_c(\cdot,\cdot)$ on the congested domain, one must have:*

$$\forall\, q \in [q_-, q_+] \quad 1+q > 0 \tag{3.5}$$

which is satisfied if and only if $q_- > -1$.

CONDITION 3.7. ***Strict hyperbolicity of the congested system.*** *In order for the congested part of* (3.2) *to be strictly hyperbolic, one must have:*

$$\forall\,(\rho,q) \in \Omega_c \quad \lambda_1(\rho,q), \lambda_2(\rho,q) \in \mathbb{R} \;\; \textit{and} \;\; \lambda_1(\rho,q) \neq \lambda_2(\rho,q).$$

Given the expression of the eigenvalues outlined in Table 3.1*, and modulo a rearrangement, this yields:*

$$\forall\,(\rho,q) \in \Omega_c \quad \rho\,\partial_\rho v_c^s(\rho) + q\,(v_c^s(\rho) + \rho\,\partial_\rho v_c^s(\rho)) \neq 0. \tag{3.6}$$

Since $v_c^s(\cdot)$ is positive and $\rho\,v_c^s(\cdot)$ is a decreasing function of ρ, this can always be satisfied for small enough values of q, and when instantiated for specific expressions of $v_c^s(\cdot)$, will result in a bound on the perturbation q.

CONDITION 3.8. ***Shape of Lax curves****. For modeling consistency, we require the* 1*-Lax curves to be LD or to have no more than one inflexion point (σ_i, q_i). In the latter case they should be concave for $\rho \leq \sigma_i$ and convex for $\rho \geq \sigma_i$. Since $\nabla\lambda_1.r_1$ is the second derivative of the* 1*-Lax curve with respect to ρ, this condition can be enforced, for any (ρ,q) in the congested domain, by checking the sign of the expression:*

$$\nabla\lambda_1.r_1 = \rho\,(2\,\partial_\rho v_c^s(\rho) + \rho\,\partial^2_{\rho\rho} v_c^s(\rho)) + q\,(2\,v_c^s + 4\,\rho\,\partial_\rho v_c^s(\rho) + \rho^2\,\partial^2_{\rho\rho} v_c^s(\rho)) \tag{3.7}$$

which has the sign of the first term for q small enough. So if $2\,\partial_\rho v_c^s(\rho)+\rho\,\partial^2_{\rho\rho} v_c^s(\rho) > 0$ the rarefaction waves go right in the (ρ,q) or $(\rho,\rho\,v)$ plane. When $v_c^s(\cdot)$ is such that $2\,\partial_\rho v_c^s(\rho) + \rho\,\partial^2_{\rho\rho} v_c^s(\rho) = 0$ the heading of rarefaction waves changes with the sign of q (it is the case for the original phase transition model), and in this case the 1*-curves are LD for $q = 0$.*
This condition consists in ensuring that expression (3.7) *is either identically zero (LD curve), or has no more than one zero and is an increasing function of the density.*

REMARK 3.9. One may note that condition 3.7 on the strict hyperbolicity of the system is satisfied whenever condition 3.6 on the positivity of speed is satisfied. Indeed equation (3.6) can be re-written as $\forall(\rho,q) \in \Omega_c \quad \rho\,\partial_\rho v_c^s(\rho)+q\partial_\rho Q_c^s(\rho) \neq 0$, which since the first term is negative, is equivalent to $\forall(\rho,q) \in \Omega_c \quad \rho\,\partial_\rho v_c^s(\rho)+q\partial_\rho Q_c^s(\rho) < 0$. For

non-zero values of $\partial_\rho Q_c^s(\rho)$, it yields $q > -\rho\,\partial_\rho v_c^s(\rho)/\partial_\rho Q_c^s(\rho) = -1 + v_c^s(\rho)/\partial_\rho Q_c^s(\rho)$ which is always satisfied when $q_- > -1$, because the second term of the right hand side is negative.

REMARK 3.10. In this model, traffic is anisotropic in the sense that no wave travels faster than vehicles ($\lambda_1(\rho, q) < \lambda_2(\rho, q) = v_c(\rho, q)$). The speed of vehicles is always positive and they stop only at maximal density.

3.3. Definition of parameters. Several parameters are used in the proposed model, which we summarize below:

(i) The free-flow speed V.
(ii) The maximal density R.
(iii) The critical density σ at standard state.
(iv) The critical density for the lower bound of the diagram σ_-.
(v) The critical density for the upper bound of the diagram σ_+.

These parameters can be identified from experimental data, and enable the definition of the parameters q_- and q_+. Figure 3.2 graphically summarizes the definition of the parameters chosen. One must note that the constraints on q_-, q_+ detailed in (3.5)-(3.6)-(3.7) translate into constraints on σ_-, σ_+, which cannot be freely chosen.

3.4. Cauchy problem. In this section we define a solution to the Cauchy problem for the system (3.2). Following [8], we use a definition derived from [4].

DEFINITION 3.11. *Given T in $\mathbb{R}_+$, u_0 in $L^1(\mathbb{R}; \Omega_f \cup \Omega_c) \cap BV(\mathbb{R}; \Omega_f \cup \Omega_c)$, an admissible solution to the corresponding Cauchy problem for (3.2) is a function $u(\cdot, \cdot)$ in $L^1([0, T] \times \mathbb{R}; \Omega_f \cup \Omega_c) \cap BV([0, T] \times \mathbb{R}; \Omega_f \cup \Omega_c)$ such that the following holds.*

(i) *For all t in $[0, T]$, $t \mapsto u(t, .)$ is Lipshitz continuous with respect to the L^1 norm.*

(ii) *For all functions φ in $C_c^1([0, T] \times \mathbb{R} \mapsto \mathbb{R})$ with compact support contained in $u^{-1}(\Omega_f)$:*

$$\int_0^T \int_{\mathbb{R}} (u(t, x)\, \partial_t \varphi(t, x) + Q_f(u(t, x)) \partial_x \varphi(t, x))\, dxdt + \int_{\mathbb{R}} u_0(x)\, \varphi(0, x) dx = 0.$$

(iii) *For all functions φ in $C_c^1([0, T] \times \mathbb{R} \mapsto \mathbb{R}^2)$ with compact support contained in $u^{-1}(\Omega_c)$:*

$$\int_0^T \int_{\mathbb{R}} (u(t, x)\, \partial_t \varphi(t, x) + Q_c(u(t, x)) \partial_x \varphi(t, x))\, dxdt + \int_{\mathbb{R}} u_0(x)\, \varphi(0, x) dx = 0.$$

(iv) *The set of points (t, x) for which there is a change of phase is the union of a finite number of Lipschitz curves $p_i : [0, T) \mapsto \mathbb{R}$ such that if $\exists i \neq j$ and $\exists \tau \in [0, T]$ such that $p_i(\tau) = p_j(\tau)$ then $\forall t \in [\tau, T]$ we have $p_i(t) = p_j(t)$.*

(v) *For all points (t, x) where there is a change of phase, let $\Lambda = \dot{p_i}(t^+)$, and introducing the left and right flow at (t, x):*

$$F^l = \begin{cases} \rho(t, x^-)\, v_f(\rho(t, x^-)) & \text{if } \rho(t, x^-) \in \Omega_f \\ \rho(t, x^-)\, v_c(\rho(t, x^-), q(t, x^-)) & \text{if } \rho(t, x^-) \in \Omega_c \end{cases}$$

$$F^r = \begin{cases} \rho(t, x^+)\, v_f(\rho(t, x^+)) & \text{if } \rho(t, x^+) \in \Omega_f \\ \rho(t, x^+)\, v_c(\rho(t, x^+), q(t, x^+)) & \text{if } \rho(t, x^+) \in \Omega_c \end{cases}$$

the following relation must be satisfied:

$$\Lambda \cdot (\rho(t, x_+) - \rho(t, x_-)) = F_r - F_l. \tag{3.8}$$

REMARK 3.12. This definition of solution matches the standard Lax entropy solution for an initial condition with values in Ω_f or Ω_c. Equation (3.8) is a Rankine-Hugoniot relation needed to ensure mass conservation at the phase transition.

THEOREM 3.13. *Let Ω_f and Ω_c be defined by* (3.4)*, $v_c(\cdot,\cdot)$ be defined by* (3.1)*. If condition 3.7 is satisfied, then for all $u_0 \in L^1(\mathbb{R};\Omega_f \cup \Omega_c) \cap BV(\mathbb{R};\Omega_f \cup \Omega_c)$ the corresponding Cauchy problem for* (3.2) *has an admissible solution, (see definition 3.11) $u(\cdot,\cdot)$ such that $u(t,\cdot) \in BV(\mathbb{R};\Omega_f \cup \Omega_c)$ for all $t > 0$.*

Proof. A solution is constructed through a standard wavefront tracking procedure by iteratively gluing together the solution to Riemann problems corresponding to piecewise constant approximations of the solution. Measuring total variation along the trajectories of these solutions allows to conclude on the convergence of the sequence of successive approximations. The interested reader is referred to [4] for more details on wavefront tracking techniques and to [8, 9] for more insights on proofs of existence for systems of conservation laws with phase transition. □

3.5. Model properties. The main differences between the original Colombo model [8] and the class of models introduced in this article result from the following design choices:

Choice of $q^* = 0$.
This is a change of variable which has several consequences. Related computations are more readable. The congested standard state is $q = 0$. According to (3.1), the meaning of the perturbation q is also more intuitive. Positive values of q correspond to elements of flow moving at a greater speed than the standard speed for this density, and negative values of q correspond to slower elements of flow. In the traffic context, this can be understood as groups of driver characterized by their degree of agressivity, q, which leads them to drive faster or slower than the standard driver.

Newell-Daganzo flux function in free-flow.
This allows the free-flow and congested domain of the fundamental diagram proposed in the present work to be connected and to define a metastable phase, as illustrated in Figure 3.3. This yields a well-posed Riemann problem which can be solved in a simple way (see Remark 2 of [8]). Moreover, the derived models need less parameters and thus are easier to calibrate. Finally, it is consistent with the fact that a gap between phases is not observed in experimental data, see Figure 3.1.

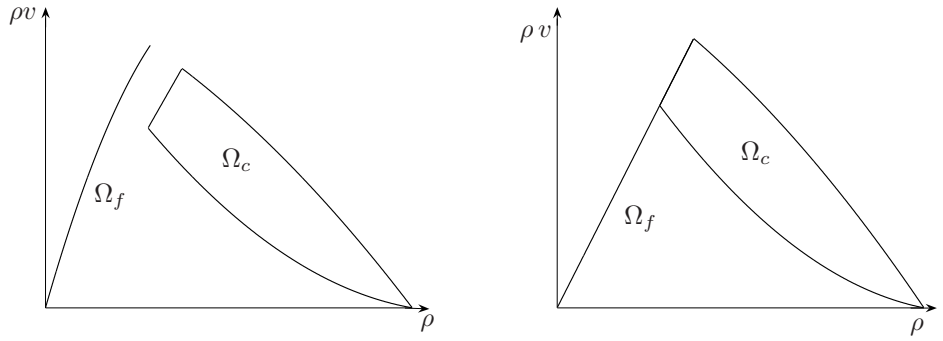

FIG. 3.3. ***Different free-flow phases. Left:*** *Fundamental diagram from the original Colombo phase transition model.* ***Right:*** *Fundamental diagram of the model derived in the present article in the particular case of a Newell-Daganzo standard state flux in the congestion phase.*

The expression of the function v_c is not fully specified.
This allows us to customize the model depending on the features observed in practice. As explained in Remark 3.14 below, the concavity of the 1-Lax curves is related to driving behavior. In the class of models we introduce, since $v_c(\cdot,\cdot)$ is not fully specified, in the limit of conditions 3.6-3.7-3.8, it is possible to define the perturbed phase transition model which corresponds to the observed driver agressivity.

REMARK 3.14. A physical interpretation can be given to the concavity of the flux function. In congestion, when the density increases toward the maximal density, the velocity decreases toward zero. This yields a decreasing slope of the flux function in congestion. The way in which drivers velocity decreases impacts the concavity of the flux, as per the expression of the second derivative of the standard flux function, $d^2Q_c^s(\rho)/d\rho^2 = \rho\, d^2v_c^s(\rho)/d\rho^2 + 2\, dv_c^s(\rho)/d\rho$.

(i) If for a given density increase, the drivers reduce their speeds more at high densities than at low densities (modeling aggressive drivers who wait until high density to reduce speed), then the velocity function is concave and the flux function is concave.

(ii) If the drivers reduce their speeds less at high densities than at low densities (modeling careful drivers who anticipate and reduce their speed early), then the velocity function is convex, and the flux function may be convex.

(iii) An affine flux is given by a velocity function which satisfies $\rho\, d^2v_c^s(\rho)/d\rho^2 + 2\, dv_c^s(\rho)/d\rho = 0$.

3.6. Numerics. Because of the non-convexity of the domain $\Omega_f \cup \Omega_c$ (illustrated in Figure 3.2), using the classical Godunov scheme [31] is not feasible due to the projection step of the scheme. We propose to use a modified version of the scheme (see [6]) which mimics the two steps of the classical Godunov scheme and adds a final sampling step.

(i) The Riemann problems are solved on a regular time space mesh. When two space-consecutive cells do not belong to the same phase, the position of the phase transition at the next time step is computed.

(ii) The solutions are averaged on the domains defined by the position of the phase transitions arising from Riemann problems at neighboring cells (Figure 3.4).

(iii) A sampling method is used to determine the value of the solution in each cell of the regular mesh.

This process answers the issues of the classical Godunov scheme with non-convex domains. Numerical results have shown that it gives accurate results on benchmark tests (we refer to [6] for more details on the test cases used).

Let us note Δt the time discretization and Δx the space discretization satisfying the *Courant-Friedrichs-Lewy* (CFL) condition [31]. We call $x_j = j\,\Delta x$ for $j \in \mathbb{Z}$ and $t^n = n\,\Delta t$ for $n \in \mathbb{N}$. We call $x_{j-1/2} = x_j - \Delta x/2$ and we define a cell $C_j^n = \{t_n\} \times [x_{j-1/2}, x_{j+1/2}[$ which has a length Δx. We call u_j^n the value of $u := (\rho, q)$ at (t_n, x_j), and, by extension, in C_j^n. The speed of the phase transition between each pair of cells (C_j^n, C_{j+1}^n) is noted $\nu_{j+1/2}^n$ ($\nu_{j+1/2}^n$ equals zero if u_j^n and u_{j+1}^n belongs to the same phase). If we call $\overline{x}_{j-1/2}^{n+1} = x_{j-1/2} + \nu_{j-1/2}^n\,\Delta t$ we can define cell $\overline{C}_j^{n+1}$ as $\overline{C}_j^{n+1} = \left\{t^{n+1}\right\} \times [\overline{x}_{j-1/2}^{n+1}, \overline{x}_{j+1/2}^{n+1}[$ which has a length $\Delta\overline{x}_j^n = \overline{x}_{j+1/2}^{n+1} - \bar{x}_{j-1/2}^{n+1}$, as shown in Figure 3.4. The solution to the Riemann problem between cells C_j^n is averaged on cells $\overline{C}_j^{n+1}$, which by construction enclose states which are either free-flowing or congested, according to the modified Godunov scheme. We define:

(i) $u_R(\nu_{j-1/2}^{n,+}, u_{j-1}^n, u_j^n)$ as the solution to the Riemann problem between u_{j-1}^n

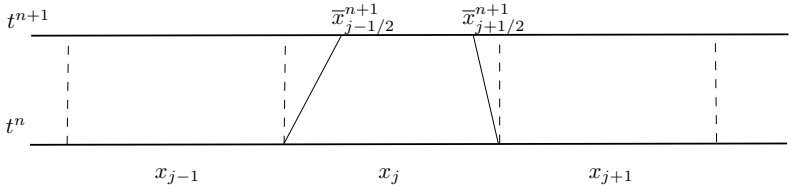

FIG. 3.4. *Phase transitions enter cell C_j^n from both sides.*

and u_j^n, at $\frac{x-x_{j-1/2}}{t-t^n} = \nu^n_{j-1/2}$, and calculated at the right of the cell boundary.

(ii) $g\left(\nu^{n,-}_{j+1/2}, u_j^n, u^n_{j+1}\right) := f(u_R(\nu^{n,-}_{j+1/2}, u_j^n, u^n_{j+1}))$ with $f(\rho, q) = (\rho\, v, q\, v)$ and the definition of v from (3.3), as the numerical flux between cells C_j^n and C_{j+1}^n, at $\frac{x-x_{j+1/2}}{t-t^n} = \nu^n_{j+1/2}$, and calculated at the left of the cell boundary.

The averaging step of the modified Godunov scheme reads:

$$\begin{aligned}\Delta\overline{x}_j^n\, \overline{u}_j^{n+1} &= \Delta x\, u_j^n - \Delta t\, \left(g\left(\nu^{n,-}_{j+1/2}, u_j^n, u^n_{j+1}\right) - \nu^n_{j+1/2}\, u_R\left(\nu^{n,-}_{j+1/2}, u_j^n, u^n_{j+1}\right)\right)\\ &+\Delta t\, \left(g\left(\nu^{n,+}_{j-1/2}, u^n_{j-1}, u_j^n\right) - \nu^n_{j-1/2}\, u_R\left(\nu^{n,+}_{j-1/2}, u^n_{j-1}, u_j^n\right)\right).\end{aligned}$$

One can notice that when there is no phase transition, $\nu^n_{j-1/2} = \nu^n_{j+1/2} = 0$, $\Delta x = \Delta\overline{x}_j^n$ and we obtain the classical Godunov scheme. The last step is the sampling phase to define the solutions on the cells C_j^{n+1}. Following [6], for cell C_j^{n+1} we randomly pick a value between $\overline{u}^{n+1}_{j-1}$, $\overline{u}^{n+1}_j$ and $\overline{u}^{n+1}_{j+1}$ according to their rate of presence in cell C_j^{n+1}. This is done using the Van der Corput sequence $(a_n)_{n\in\mathbb{N}}$ (3.9) which is a low-discrepancy sequence in the interval $[0, 1]$:

$$u_j^{n+1} = \begin{cases} \overline{u}^{n+1}_{j-1} & \text{if } a_n \in]0, \max(\frac{\Delta t}{\Delta\overline{x}_j^n}\, \nu^n_{j-1/2}, 0)]\\ \overline{u}^{n+1}_j & \text{if } a_n \in] \max(\frac{\Delta t}{\Delta\overline{x}_j^n}\, \nu^n_{j-1/2}, 0), 1 + \min(\frac{\Delta t}{\Delta\overline{x}_j^n}\, \nu^n_{j+1/2}, 0)[\\ \overline{u}^{n+1}_{j+1} & \text{if } a_n \in [1 + \min(\frac{\Delta t}{\Delta\overline{x}_j^n}\, \nu^n_{j+1/2}, 0), 1[\end{cases} \tag{3.9}$$

REMARK 3.15. In the general case the congested domain Ω_c is not convex in (ρ, q) coordinates due to the convexity of the metastable border of the domain as illustrated on Figure 3.2. It is therefore needed to add a projection step as a fourth step to the modified Godunov scheme. The projected state (ρ_p, q_p) of state (ρ, q) is defined as the solution in the metastable phase of the system:

$$\begin{cases} \frac{q_p}{\rho_p} = \frac{q}{\rho}\\ v_c(\rho_p, q_p) = V\end{cases}$$

The error metric chosen to assess the numerical accuracy of the scheme is the $C^0(\mathbb{R}, L^1(\mathbb{R}, \mathbb{R}^2))$ relative error between the computed solution and the analytical solution. We call u and u_c the exact and computed solutions respectively. For the computational domain $[x_0, x_1]$, the error at T is computed as follows:

$$E(T) = \frac{\sup_{t\in[0,T]} \int_{x_0}^{x_1} \|u(t,x) - u_c(t,x)\|_1 dxdt}{\sup_{t\in[0,T]} \int_{x_0}^{x_1} \|u(t,x)\|_1 dxdt}.$$

4. The Newell-Daganzo phase transition model. In this section, we use a Newell-Daganzo velocity function for congestion, i.e. a velocity function for which the flux is affine with respect to the density. We instantiate the corresponding (ρ, q) model for this flux function and derive a corresponding Riemann solver, which we implement and test on a benchmark case.

4.1. Analysis. We propose to use the following standard velocity function:

$$v_c^s(\rho) = \frac{V\,\sigma}{R-\sigma}\left(\frac{R}{\rho}-1\right),$$

which is clearly the unique function yielding an affine flux, and satisfying the requirements from Section § 3.1, on the vanishing point, trend, continuity and concavity property of the standard flux.

For a perturbed state, the velocity function reads:

$$\begin{cases} v_f(\rho) = V & \text{for } (\rho,q)\in\Omega_f \\ v_c(\rho,q) = \frac{V\,\sigma}{R-\sigma}\left(\frac{R}{\rho}-1\right)(1+q) & \text{for } (\rho,q)\in\Omega_c \end{cases} \tag{4.1}$$

where Ω_f and Ω_c are defined by (3.4). The corresponding fundamental diagram is shown in Figure 3.2. The standard flux is affine with the density, but the 1-Lax curves outside the standard state are either convex or concave in $(\rho, \rho\, v)$ coordinates depending on the sign of the perturbation.

REMARK 4.1. Note that the expression of the velocity in Figure 3.2 is given by (4.1), depends on the phase, and is therefore set-valued for $\rho > \sigma_-$ which is the lowest density value at which congestion can arise.

The conditions from Section § 3.2 to have positive speed and strict hyperbolicity of the congested part of the system (3.2) reduce to:

$$q_- > -1.$$

4.2. Solution to the Riemann problem. Following [8],we construct the solution to the Riemann problem for the system (3.2) with the velocity function defined by (4.1) and the initial datum:

$$(\rho,q)(0,x) = \begin{cases} (\rho_l, q_l) & \text{if } x<0 \\ (\rho_r, q_r) & \text{if } x>0. \end{cases}$$

We note u the vector (ρ, q). We define u_m by the solution in Ω_c of the system:

$$\begin{cases} \frac{q_m}{\rho_m} = \frac{q_l}{\rho_l} \\ v_c(u_m) = v_c(u_r) \end{cases} \tag{4.2}$$

which yields a quadratic polynomial in ρ_m. We address the general case where the solution u_m of system (4.2) can coincide with u_l or u_r.

Case 1: $u_l \in \Omega_f$ and $u_r \in \Omega_f$
For all values of (ρ_l, ρ_r) the solution consists of a contact discontinuity from u_l to u_r.

Case 2: $u_l \in \Omega_c$ and $u_r \in \Omega_c$

(i) If $q_l > 0$ and $v_c(u_r) \geq v_c(u_l)$ the solution consists of a 1-rarefaction wave from u_l to u_m and a 2-contact discontinuity from u_m to u_r.

(ii) If $q_l > 0$ and $v_c(u_l) > v_c(u_r)$ the solution consists of a shock wave from u_l to u_m and a 2-contact discontinuity from u_m to u_r.

(iii) If $q_l = 0$ the solution consists of a 1-contact discontinuity from u_l to u_m and a 2-contact discontinuity from u_m to u_r.

(iv) If $0 > q_l$ and $v_c(u_r) > v_c(u_l)$ the solution consists of a shock wave from u_l to u_m and a 2-contact discontinuity from u_m to u_r.

(v) If $0 > q_l$ and $v_c(u_l) \geq v_c(u_r)$ the solution consists of a 1-rarefaction wave from u_l to u_m and a 2-contact discontinuity from u_m to u_r.

Case 3: $u_l \in \Omega_c$ and $u_r \in \Omega_f$

(i) If $0 > q_l$ the solution consists of a shock wave from u_l to u_m and of a contact-discontinuity from u_m to u_r.

(ii) If $q_l = 0$ the solution consists of a 1-contact discontinuity from u_l to u_m and of a contact-discontinuity from u_m to u_r.

(iii) If $q_l > 0$ the solution consists of a 1-rarefaction wave from u_l to u_m and of a contact-discontinuity from u_m to u_r.

Case 4: $u_l \in \Omega_f$ and $u_r \in \Omega_c$ Let u_{m-} be defined by the solution in Ω_c of the system:

$$\begin{cases} \frac{q_{m-}}{\rho_{m-}} = \frac{q_-}{R} \\ v_c(u_{m-}) = v_c(u_r) \end{cases}$$

and let $\Lambda(u_l, u_{m-})$ be the Rankine-Hugoniot phase transition speed between u_l and u_{m-} defined by equation (3.8).

(i) If $\Lambda(u_l, u_{m-}) \geq \lambda_1(u_{m-})$ the solution consists of a phase transition from u_l to u_{m-} and of a 2-contact discontinuity from u_{m-} to u_r.

(ii) If $\Lambda(u_l, u_{m-}) < \lambda_1(u_{m-})$ let u_p be defined by the solution in Ω_c of the system:

$$\begin{cases} \frac{q_p}{\rho_p} = \frac{q_-}{R} \\ \Lambda(u_l, u_p) = \lambda_1(u_p). \end{cases}$$

The solution consists of a phase transition from u_l to u_p, of a 1-rarefaction wave from u_p to u_{m-}, and of a 2-contact discontinuity from u_{m-} to u_r.

4.3. Model properties. The properties of the Newell-Daganzo model can be abstracted from the definition of the Riemann solver in previous Section.

The nature of the Lax curves in congestion is the same for the original Colombo model and the Newell-Daganzo phase transition model (see Figure 3.3). Thus the solution for each model differ only when a free-flow state is involved. Three differences appear in that case:

- For a given density corresponding to the free-flow phase, the associated velocity differ in general between the two models.
- Within the free-flow phase, only contact discontinuity can arise in the Newell-Daganzo phase transition model, whereas rarefaction waves and shockwaves can arise in the original Colombo model.
- A transition from congestion to free-flow always involves a shock-like phase transition in the Colombo model (and thus the solution is composed of three waves in general), whereas the transition occurs through a metastable state in the Newell-Daganzo phase transition model, and involves only a "congestion to metastable" wave and a "metastable to free-flow" wave.

These properties are illustrated in the next Section on a Riemann problem.

As in the original Colombo phase transition model [8], the 1-Lax curves are LD for $q = 0$, and the direction of the rarefaction waves changes according to the sign of q. This yields interesting modeling capabilities, but requires the Riemann solver to be more complex than the one described in the following Section.

REMARK 4.2. As illustrated on Figure 3.2 the flux is linear in congestion at the standard state as per the Newell-Daganzo flux function. Remark 3.14 states that this shape models neutral drivers (aggressivity-wise). When the traffic is above the standard state, meaning that the velocity is higher that what it is for the same density at the standard state, the 1-Lax curves are concave in $(\rho, \rho\, v)$ coordinates, meaning that the drivers are more aggressive. So such a fundamental diagram shape seems to be in accordance with the intuition, that for a given density, the most aggressive drivers tend to have a greater speed. This is symmetrically true for less aggressive drivers, also accounted for by this model.

4.4. Benchmark test. In this section we compare the numerical solution given by the modified Godunov scheme with the analytical solution to a Riemann problem. We use the phase transition model (3.2) in the Newell-Daganzo case (4.1) with the following choice of parameters: $V = 45$, $R = 1000$, $\sigma_- = 190$, $\sigma = 220$, $\sigma_+ = 270$. The benchmark test is a phase transition from congestion to free-flow with the following left and right states:

(i) $u_l = (800, -0.1)$ which corresponds to congestion below standard state with $\rho = 800$ and $v = 2.9$.

(ii) $u_r = (100, 0)$ which corresponds to a free-flow state with $\rho = 100$ and $v = 45$.

This configuration gives rise to a shock wave between u_l and a congested state u_m followed by a contact discontinuity between u_m and u_r (Riemann case 3, first subcase), as shown in Figure 4.1.

We also present the solution given by the original Colombo model with the following parameters: $V_{c+} = 45$, $V_{f-} = 57$, $V = 67$, $q^* = 0$, $Q^- = -0.88$ and $Q^+ = 1.15$. The congested phases in the two models are identical with this choice of parameters. One may note that because the fundamental diagram in free-flow differs between the original Colombo model and the Newell-Daganzo phase transition model (see Figure 3.3), the speed corresponding to the right initial state in the Riemann problem is greater in the Colombo model.

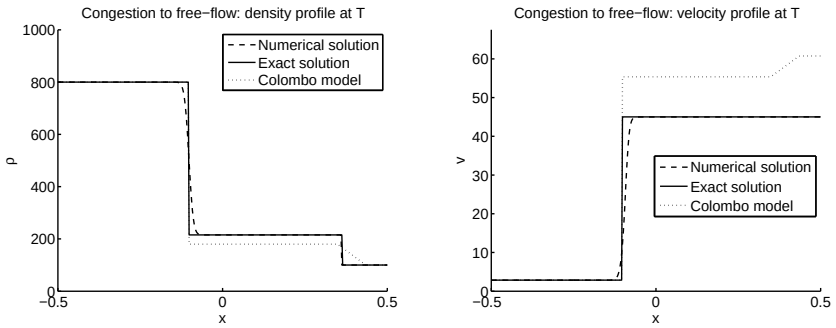

FIG. 4.1. *Exact solution (continuous line), computed solution (dashed line), and exact solution for the Colombo model (dotted line) for density (left) and speed (right). Between the two initial states, for the class of models presented in this article, appears a state* $u_m = (215.4, -0.03)$ *which corresponds to the intersection of the 1-Lax curve going through* u_l *with the metastable phase. In this graph* $T = 0.4$ *and* $\Delta x = 0.0013$.

The solutions to the Riemann problem for each model differ on several points. First the intermediary state u_m belongs to the metastable phase in the Newell-Daganzo model whereas it belongs to the free-flow phase for the Colombo model. Second the wave from the intermediary state u_m to the right state u_r is a rarefaction wave in the Colombo model, as illustrated in Figure 4.1, whereas it is a contact discontinuity in the Newell-Daganzo phase transition model.

The values of the error $E(T)$, as described in Section § 3.6 for $T = 4$, (a typical time for which all interactions have moved out of the computational domain) are outlined in Table 4.1.

Cell ♯	$E(T)$
50	$5.8\ 10^{-04}$
100	$2.0\ 10^{-04}$
200	$6.4\ 10^{-05}$
400	$2.0\ 10^{-05}$

TABLE 4.1

Numerical error: *relative error between exact solution and the modified Godunov scheme solution for the benchmark described above, for different discretizations.*

5. The Greenshields phase transition model. In this section we use a Greenshields model to describe the velocity function in congestion, i.e. we use a concave quadratic flux function. We present the standard and perturbed flux functions, derive the corresponding Riemann solver which we test on a benchmark case, and describe the properties of the Greenshields phase transition model.

5.1. Analysis. We use a quadratic relation to describe the congestion standard state, which for physical considerations needs to satisfy the requirements from Section § 3.1. This leads us to choose the flux as a quadratic function of the form:

$$\rho\, v_c^s(\rho) = (\rho - R)\,(a\,\rho + b)$$

such that the vanishing condition at $\rho = R$ is satisfied. Continuity at the critical density σ yields:

$$b = \frac{\sigma\, V}{\sigma - R} - a\,\sigma$$

so the flux at the standard state reads:

$$\rho\, v_c^s(\rho) = (\rho - R)\,\left(a\,(\rho - \sigma) + \frac{\sigma\, V}{\sigma - R}\right)$$

with a variation interval for a defined by the second and third conditions of Section § 3.1 as:

$$a \in \left[-\frac{\sigma\, V}{(\sigma - R)^2}, 0\right[\,.$$

Note that for the specific case in which $R = 2\,\sigma$ and a is defined by the fact that the derivative of the flux equals zero at σ (which reads $a = -\sigma\, V/(\sigma - R)^2$), we obtain the classical Greenshields flux.

Following the general form given in system (3.3), we write the perturbed velocity function as:

$$\begin{cases} v_f(\rho) = V & \text{for } (\rho, q) \in \Omega_f \\ v_c(\rho, q) = \left(1 - \frac{R}{\rho}\right) \left(a\,(\rho - \sigma) + \frac{\sigma\, V}{\sigma - R}\right) (1 + q) & \text{for } (\rho, q) \in \Omega_c \end{cases} \tag{5.1}$$

with $a \in \left[-\frac{\sigma\, V}{(\sigma - R)^2}, 0\right[$, and where Ω_f and Ω_c are defined by (3.4). The corresponding fundamental diagram is presented in Figure 5.1.

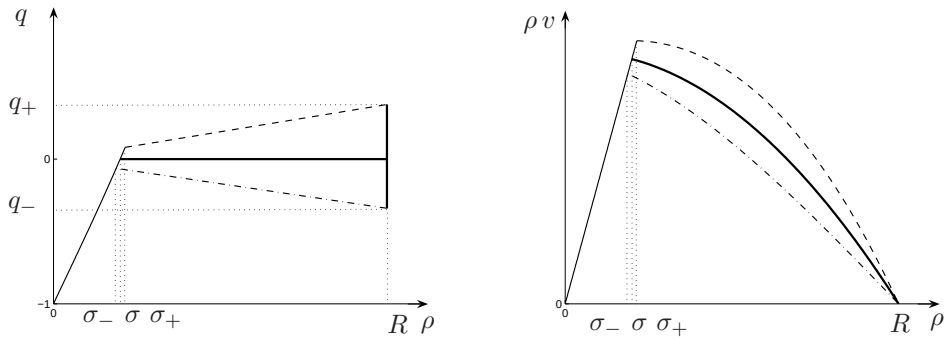

FIG. 5.1. ***Phase transition model with a Greenshields standard state. Left:*** *State-space coordinates.* ***Right:*** *Flux-density coordinates. Thin solid line: Free-flow. Bold solid line: Congestion standard state. Thin dashed line: Upper bound of congestion. Thin dot-dashed line: Lower bound of congestion. The standard flux is concave, and all the 1-Lax curves are concave in* $(\rho, \rho\, v)$ *coordinates. In* (ρ, q) *coordinates the free-flow phase is not a straight line but has a very light convexity.*

REMARK 5.1. The expression of the velocity function given by system (5.1) enables a set-valued velocity function for $\rho > \sigma_-$. For a given density the variable velocity can take several values. The lower bound of congestion is concave, unlike for the model presented in Section § 4. This feature may be more appropriate for usual experimental datasets.

The requirements from Section § 3.2 here reduce to:

$$q_- > -\frac{a\, R}{\frac{\sigma\, V}{\sigma - R} + a\,(2\, R - \sigma)}.$$

While in the Newell-Daganzo phase transition model the bound on the perturbation was given by the fact that the speed had to be positive, here the bound is given by the requirement on the constant concavity of the 1-Lax curves.

REMARK 5.2. The lower bound on the perturbation is an increasing function of the parameter a, so this parameter should be chosen as small as possible to allow for more freedom, namely $a_{\min} = -\sigma\, V/(\sigma - R)^2$ which yields the lowest lower bound bound $q_-^{\min} = R/(2\,\sigma - 3\, R)$.

5.2. Solution to the Riemann problem. We consider the Riemann problem for system (3.2) with the velocity function from equation (5.1) and the initial datum:

$$(\rho, q)(0, x) = \begin{cases} (\rho_l, q_l) & \text{if } x < 0 \\ (\rho_r, q_r) & \text{if } x > 0. \end{cases} \tag{5.2}$$

We follow the method used in [8] to construct the solution. We define u_m by the solution in Ω_c of the system:

$$\begin{cases} \frac{q_m}{\rho_m} = \frac{q_l}{\rho_l} \\ v_c(u_m) = v_c(u_r) \end{cases} \tag{5.3}$$

which yields a quadratic polynomial in ρ_m with one root in $[0, R]$. In the general case, the solution u_m of the system (5.3) can be equal to u_l or u_r.

Case 1: $u_l \in \Omega_f$ and $u_r \in \Omega_f$ For all values of (ρ_l, ρ_r) the solution consists of a contact discontinuity from u_l to u_r.

Case 2: $u_l \in \Omega_c$ and $u_r \in \Omega_c$

(i) If $v_c(u_r) \geq v_c(u_l)$ the solution consists of a 1-rarefaction wave from u_l to u_m and a 2-contact discontinuity from u_m to u_r.

(ii) If $v_c(u_l) > v_c(u_r)$ the solution consists of a shock wave from u_l to u_m and a 2-contact discontinuity from u_m to u_r.

Case 3: $u_l \in \Omega_c$ and $u_r \in \Omega_f$ The solution consists of a 1-rarefaction wave from u_l to u_m and of a contact-discontinuity from u_m to u_r.

Case 4: $u_l \in \Omega_f$ and $u_r \in \Omega_c$ Let u_{m-} be defined by the solution in Ω_c of the system:

$$\begin{cases} \frac{q_{m-}}{\rho_{m-}} = \frac{q_-}{R} \\ v_c(u_{m-}) = v_c(u_r). \end{cases}$$

The solution consists of a phase transition from u_l to u_{m-} and of a 2-contact discontinuity from u_{m-} to u_r.

REMARK 5.3. The analysis in the case of a convex standard flux function, which we do not address in this article, is closely related to this case, modulo the sign of the parameter a and the concavity of the 1-Lax curves.

5.3. Model properties. The structure of the solution to the Riemann problem presented in previous section explains the distinction with the original phase transition model:

- Since the 1-Lax curves are concave, within the congestion phase, shock waves occur only from a low density on the left to a high density on the right. This is similar to classical traffic models with concave flux.
- The concavity of the 1-Lax curves yields simple transitions from a free-flow state to a congested state. These phase transitions are composed of a shock-like phase transition followed by a contact discontinuity, whereas a rarefaction wave can appear between the two in the original phase transition model or in the Newell-Daganzo phase transition model.
- Similarly to the Newell-Daganzo phase transition model, within the free-flow phase, the Greenshield phase transition model exhibits only contact discontinuities.

Another consequence of the fact that the 1-Lax curves are concave is that the Riemann solver is much simpler than in the Newell-Daganzo case, with only five different types of solutions, compared to the Newell-Daganzo case which has eleven different types of solutions.

REMARK 5.4. According to Remark 3.14 this flux function models aggressive drivers only, who drive along concave 1-Lax curves. In practice, it is able to model a class of clouds of points observed experimentally where the congested domain has a concave lower border in $(\rho, \rho\, v)$ coordinates.

5.4. Benchmark test. In this section we compare the numerical results given by the modified Godunov scheme on a benchmark test with its analytical solution. We use the phase transition model (3.2) in the Greenshields case (5.1) with the following choice of parameters: $V = 45$, $R = 1000$, $\sigma_- = 190$, $\sigma = 200$, $\sigma_+ = 215$. We choose $a = -0.01$. The resulting values for the extrema of the perturbation are $q_- = -0.34$ and $q_+ = 0.44$. The benchmark test is a phase transition from free-flow to congestion, with the following left and right states:

(i) $u_l = (180, 0)$ which corresponds to a free-flow state with $\rho = 180$ and $v = 45$.

(ii) $u_r = (900, 0.2)$ which corresponds to a congested situation above standard state with $\rho = 900$ and $v = 2.4$.

This configuration gives rise to a phase transition between u_l and a congested state u_m followed by a 2-contact discontinuity between u_m and u_r (Riemann case 4) which is illustrated in Figure 5.2.

We also present the solution to the Riemann problem for the original Colombo model with parameters: $V_{c+} = 45$, $V_{f-} = 57$, $V = 67$, $q^* = 0$, $Q^- = -0.32$ and $Q^+ = 0.44$. The speed in free-flow differs between the two models. The phase transition speed is negative for both models but is smaller in absolute value in the case of the Greenshields phase transition model which models more aggressive drivers which have a higher flux in congestion for the same density value. The second wave has the same speed in the two models.

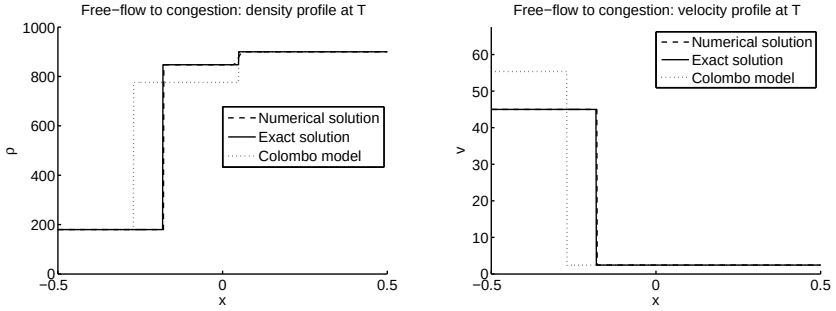

FIG. 5.2. *Exact solution (continuous line), computed solution (dashed line), and solution to the Colombo model (dotted line) for density (left) and speed (right). Between the two initial states appears a state* $u_m = (847.4, -0.24)$ *which corresponds to the intersection of the lower bound of the diagram in congestion with the 2-Lax curve going through* u_r*. In this graph* $T = 1$ *and* $\Delta x = 0.0013$*.*

Table 5.1 summarizes the values of the error $E(T)$, as defined in Section § 3.6, for different sizes of the discretization step, at $T = 4$.

Cell ♯	$E(T)$
50	$3.1\ 10^{-04}$
100	$7.8\ 10^{-05}$
200	$2.1\ 10^{-05}$
400	$5.4\ 10^{-06}$

TABLE 5.1

Relative error between exact solution and numerical solution for the test case explicitly described above, for different numbers of space cells.

6. Conclusion. This article reviewed the fundamental features of the Colombo phase transition model and proposed to build upon it a class of models in which the

fundamental diagram is set-valued in the congested regime. The notion of standard state which provides the basis for the construction of the 2×2 phase transition models was introduced. General conditions which enable the extension of the original Colombo phase transition model to this new class of 2×2 phase transition models were investigated. A modified Godunov scheme which can be applied to models with non-convex state-space was used to solve these equations numerically. The model was instantiated for two specific flux functions, which include the Newell-Daganzo flux function (affine) and the Greenshields flux function (quadratic concave). A discussion of the choice of parameters needed for each of the models was conducted. The solution to the Riemann problem was derived, and a validation of the numerical results using benchmark tests was conducted. Open questions for this model include the capability of the model to accurately reproduce traffic features experimentally measured on highways. Experimental validations of the model should reveal its capabilities of reproducing traffic flow more accurately than existing models. In addition, the specific potential of the model to integrate velocity measurements (through proper treatment of the second state variable of the problem) is a significant advantage of this model over any first order model for which the density-flux relation is single valued. The proper use of this key feature for data assimilation is also an open problem, which could have very promising outcomes for highway traffic state estimation.

REFERENCES

[1] A. Aw and M. Rascle, *Resurrection of "second order" models of traffic flow*, SIAM J. Appl. Math., 60 (2000), pp. 916–938.

[2] C. Bardos, A.-Y. Leroux, and J.-C. Nedelec, *First order quasilinear equations with boundary conditions*, Comm. Partial Differential Equations, 4 (1979), pp. 1017–1034.

[3] S. Blandin, G. Bretti, A. Cutolo, and B. Piccoli, *Numerical simulations of traffic data via fluid dynamic approach*, Applied Mathematics and Computation, 210 (2009), pp. 441–454.

[4] A. Bressan, *Hyperbolic systems of conservation laws: the one-dimensional Cauchy problem*, Oxford University Press, 2000.

[5] M. Cassidy and J. Windover, *Methodology for assessing dynamics of freeway traffic flow*, Transportation Research Record, 1484 (1995), pp. 73–79.

[6] C. Chalons and P. Goatin, *Godunov scheme and sampling technique for computing phase transitions in traffic flow modeling*, Interfaces and Free Boundaries, 10 (2008), pp. 195–219.

[7] R. Colombo, *On a 2×2 hyperbolic traffic flow model*, Math. Comput. Modelling, 35 (2002), pp. 683–688.

[8] ———, *Hyperbolic phase transitions in traffic flow*, SIAM J. Appl. Math., 63 (2003), pp. 708–721.

[9] R. Colombo, P. Goatin, and F. Priuli, *Global well-posedness of traffic flow models with phase transitions*, Nonlinear Analysis, 66 (2007), pp. 2413–2426.

[10] C. Daganzo, *The cell transmission model: a dynamic representation of highway traffic consistent with the hydrodynamic theory*, Transportation Research Part B, 28 (1994), pp. 269–287.

[11] ———, *The cell transmission model, part ii: Network traffic*, Transportation Research Part B, 29 (1995), pp. 79–93.

[12] ———, *Requiem for second-order fluid approximations of traffic flow*, Transportation Research Part B, 29 (1995), pp. 277–286.

[13] C. Daganzo, M. Cassidy, and R. Bertini, *Possible explanations of phase transitions in highway traffic*, Transportation Research Part A, 33 (1999), pp. 365–379.

[14] J. Del Castillo and F. Benitez, *On the functional form of the speed-density relationship i: General theory*, Transportation Research Part B, 29 (1995), pp. 373–389.

[15] J. Del Castillo, P. Pintado, and F. Benitez, *The reaction time of drivers and the stability of traffic flow*, Transportation research. Part B, 28 (1994), pp. 35–60.

[16] M. Garavello and B. Piccoli, *Traffic flow on networks*, American Institute of Mathematical Sciences, 2006.

[17] ———, *On fluido-dynamic models for urban traffic*, Netw. Heterog. Media, 4 (2009), pp. 107–

126.
[18] J. Glimm, *Solutions in the large for nonlinear hyperbolic systems of equations*, Comm. Pure Appl. Math., 18 (1965), pp. 697–715.
[19] P. Goatin, *The Aw-Rascle vehicular traffic flow model with phase transitions*, Math. Comput. Modelling, 44 (2006), pp. 287–303.
[20] S. Godunov, *A difference method for numerical calculation of discontinuous solutions of the equations of hydrodynamics*, Sb. Math., 89 (1959), pp. 271–306.
[21] H. Greenberg, *An analysis of traffic flow*, Oper. Res., 7 (1959), pp. 79–85.
[22] B. Greenshields, *A study of traffic capacity*, Proceedings of the Highway Research Board, 14 (1935), pp. 448–477.
[23] H. Holden and N. Risebro, *Front tracking for hyperbolic conservation laws*, Springer-Verlag, 2002.
[24] Z. Jia, C. Chen, B. Coifman, and P. Varaiya, *The PeMS algorithms for accurate, real-time estimates of g-factors and speeds from single-loop detectors*, in Intelligent Transportation Systems, 2001, pp. 536–541.
[25] B. Kerner, *Experimental features of self-organization in traffic flow*, Phys. Rev. Lett., 81 (1998), pp. 3797–3800.
[26] ———, *Phase transitions in traffic flow*, Traffic and granular flow, (2000), pp. 253–283.
[27] S. Kruzhkov, *First order quasilinear equations in several space variables*, Sb. Math., 10 (1970), pp. 217–243.
[28] L. Tong, *Nonlinear dynamics of traffic jams*, Phys. D, 207 (2005), pp. 41–51.
[29] J. Lebacque, *The Godunov scheme and what it means for first order macroscopic traffic flow models*, Proceedings of the 13th ISTTT, Ed. J.B. Lesort,, (Lyon, 1996), pp. 647–677.
[30] P. Le Floch, *Explicit formula for scalar non-linear conservation laws with boundary conditions*, Mathematical methods in the applied sciences, 10 (1988), pp. 265–287.
[31] R. Leveque, *Finite volume methods for hyperbolic problems*, Cambridge University Press, 1992.
[32] M. Lighthill and G. Whitham, *On kinematic waves ii a theory of traffic flow on long crowded roads*, Proc. R. Soc. Lond. Ser. A Math. Phys. Eng. Sci., 229 (1956), pp. 317–345.
[33] W. Lin and D. Ahanotu, *Validating the basic cell transmission model on a single freeway link*, tech. report, Institute of Transportation Studies, University of California, Berkeley, 1995.
[34] L. Munoz, X. Sun, R. Horowitz, and L. Alvarez, *Traffic density estimation with the cell transmission model*, in American Control Conference, 2003. Proceedings of the 2003, vol. 5, 2003.
[35] G. Newell, *A simplified theory of kinematic waves in highway traffic ii: Queueing at freeway bottlenecks*, Transportation research Part B, 27 (1993), pp. 289–303.
[36] O. Oleinik, *Discontinuous solutions of non-linear differential equations*, Uspekhi Mat. Nauk, 12 (1957), pp. 3–73.
[37] M. Papageorgiou, *Some remarks on macroscopic traffic flow modelling*, Transportation Research Part A, 32 (1998), pp. 323–329.
[38] H. Payne, *Models of freeway traffic and control*, Simulation Councils, Inc., 1971.
[39] P. Richards, *Shock waves on the highway*, Oper. Res., 4 (1956), pp. 42–51.
[40] D. Serre, *Systems of conservation laws*, Diderot, 1996.
[41] I. Strub and A. Bayen, *Weak formulation of boundary conditions for scalar conservation laws: an application to highway traffic modelling*, Internat. J. Robust Nonlinear Control, 16 (2006), pp. 733–748.
[42] B. Temple, *Systems of conversation laws with invariant submanifolds*, Trans. Amer. Math. Soc., 280 (1983), pp. 781–795.
[43] E. Toro, *Riemann solvers and numerical methods for fluid dynamics*, Springer-Verlag, 1997.
[44] R. Underwood, *Speed, volume, and density relationships: Quality and theory of traffic flow*, Yale Bureau of Highway Traffic, (1961), pp. 141–188.
[45] P. Varaiya, *Reducing highway congestion: an empirical approach*, Eur. J. Control, 11 (2005), pp. 301–309.
[46] ———, *Congestion, ramp metering and tolls*, Philos. Trans. R. Soc. Lond. Ser. A Math. Phys. Eng. Sci., 366 (2008), pp. 1921–1930.
[47] Y. Wang and M. Papageorgiou, *Real-time freeway traffic state estimation based on extended kalman filter: a general approach*, Transportation Research Part B, 39 (2005), pp. 141–167.
[48] G. Whitham, *Linear and Nonlinear Waves*, Pure Appl. Math., 1974.
[49] H. Zhang, *A theory of nonequilibrium traffic flow*, Transportation Research Part B, 32 (1998), pp. 485–498.
[50] ———, *A non-equilibrium traffic model devoid of gas-like behavior*, Transportation Research Part B, 36 (2002), pp. 275–290.